Space Engineering

Space Propulsion Project: Design Of a Liquid Propulsion Unit

POLITECNICO
MILANO 1863

Team: Pink Origin

Mads L. U. Larsen	984967
Francesco Salvaterra	988375
Daniela Pacifici	992298
Francesca Tozzini	996623
Riccardo Severi	992041
Federico Infantino	996989
Bruno Falo	100861
Gloria Castronovo	992130
Antonio Guerriero	991852

Space Propulsion - 2021/2022

Prof. Filippo Maggi

Abstract

The aim of this work is to design a blowdown configuration liquid rocket engine providing a nominal thrust of 100 N. Then its behaviour during the firing time will be simulated in order to evaluate its performances over time and assure at least the 50% of the nominal thrust at the end of the firing. It will be study the feasibility using technique from additive manufacturing and a qualitative discussion will be extended to a smaller engine of 10 N and a larger one of 1000 N. A Monte Carlo analysis based on the nominal design will be performed in order to take into account the uncertainties mainly coming from additive manufacturing.

Preface

This project is written in LaTeX. The Harvard method is used for source reference.

Nomenclature

Symbols

σ_U	Standard deviation
α	Convergent part angle of the nozzle
β	Divergent part angle of the nozzle
$\dot{m_{fu}}$	Fuel mass flow rate
$\dot{m_{ox}}$	Oxidizer mass flow rate
$\dot{m}_p$	Propellant mass flow rate
$\dot{m}$	Mass flow rate
$\dot{V}_{ox}$	Oxidizer volumetric flow rate
ϵ	Expansion ratio
$\Gamma(k)$	Vandekerkhove function
λ	Loss coefficient of the nozzle
ρ	Fluid (oxidizer or fuel) density
ρ_{tank}	Density of the tank material (stainless steel 316)
θ_e	Exit angle of the parabolic approximation
θ_i	Initial angle of the parabolic approximation
A_b	Combustion chamber section for the reference conical nozzle
A_{cc}	Combustion chamber cross section area
B	Blow-down ratio
c^*	Characteristic velocity
c_T	Thrust coefficient
d_e	Exit diameter
d_t	Throat diameter
D_{line}	Feeding line diameter
f	Pipe friction factor
g_0	Earth gravitational acceleration at sea level
I_s	Specific impulse
K	Pressure loss coefficient
k	Heat capacity ratio
L	Fluid (oxidizer or fuel) pipe length
L^*	Characteristic length
L_{cc}	Combustion chamber length
L_{conv}	Convergent part length of the nozzle
L_{div}	Divergent part length of the nozzle
L_{nozzle}	Nozzle total length
L_{RAO}	Rao conical nozzle total length
M	Molar mass of the propellant
M_c	Mach number inside the combustion chamber, equal at any point
M_{fu}	Fuel mass
M_{ox}	Oxidizer mass
OF	Oxidizer to fuel ratio
p_a	Ambient pressure
p_c	Combustion chamber pressure
p_e	Exit pressure
p_{blast}	Blast pressure
$p_{tank,fu}$	Fuel tank pressure
$p_{tank,ox}$	Oxidizer tank pressure
R	Universal gas constant

t_{burn}	Burning time
T_{cc}	Combustion chamber temperature
T_{melt}	Melting temperature of the combustion chamber material, Inconel 718
T_{real}	Real thrust of the engine
v	Fluid (oxidizer or fuel) velocity in the pipe
v_e	Flow exit velocity
V_{cc}	Combustion chamber volume
v_e	Exit velocity of the flow
V_f	Fuel volume
V_{ox}	Oxidizer volume
ΔP	Pressure drop
γ_f	Angle of the fuel injector
σ	Yield strength
A	Diameter of orifices
C_d	Discharge coefficient
d_{inj}	Injector orifice diameter
K_v	flow coefficient
n_{inj}	Number of injectors
q_v	volumetric flow rate
v_f	Discharge velocity of the fuel flow
$V_{in,PG,f}$	Initial volume of the pressurizing gas for the fuel
$V_{in,PG,ox}$	Initial volume of the pressurizing gas for the oxidizer
v_{ox}	Discharge velocity of the oxidizer flow
$V_{tank,f}$	Volume of the fuel tank
$V_{tank,ox}$	Volume of the oxidizer tank

Abstract

The aim of this work is to design a blowdown configuration liquid rocket engine providing a nominal thrust of 100 N. Then its behaviour during the firing time will be simulated in order to evaluate its performances over time and assure at least the 50% of the nominal thrust at the end of the firing. It will be study the feasibility using technique from additive manufacturing and a qualitative discussion will be extended to a smaller engine of 10 N and a larger one of 1000 N. A Monte Carlo analysis based on the nominal design will be performed in order to take into account the uncertainties mainly coming from additive manufacturing.

Contents

Introduction 1

1.1 Nozzle design and nominal performances

The identification of the nominal O/F ratio is done through a CEA Analysis considering a range of O/F values between 5 and 8.5 (typical of the couple RP-1 - H_2O_2), the given combustion chamber pressure and the expansion ratio (see Appendix A). As showed in Figure C.1, the highest specific impulse is reached with an oxidizer to fuel ratio value of 7. It is necessary to estimate the temperature reached inside the combustion chamber, value that must be compliant with the choice of the constructive material: Inconel 718 with a T_{melt}= 1643 K to 1703 K.

Since the value of the temperature reached inside the combustion chamber (2656.8 K) is higher with respect to the melting point of the alloy, a regenerative cooling system that can guarantee the correct behaviour of the motor is considered to be present. The nominal oxidizer to fuel ratio is set to $OF = 7$.

From CEA analysis the thermodynamics and physical parameters of the propellant mixture are retrieved:

k [-]	T_{cc} [K]	M [kg/mol]
1.1811	2656.8	21.833

Table 1.1: Propellant properties

The characteristic velocity and the thrust coefficient are computed through Eq. (1.1) and Eq. (1.3).

$$C_T = \sqrt{\frac{2k^2}{k-1}\left(\frac{2}{k+1}\right)^{\frac{k+1}{k-1}}}\sqrt{1-\left(\frac{P_e}{P_c}\right)^{\frac{k-1}{k}}} + \left(\frac{P_e - P_a}{P_c}\right)\frac{A_e}{A_t} = 1.9676 \tag{1.1}$$

Where $P_a = 0$ is the ambient pressure (vacuum) and P_e is the exit pressure of the nozzle, obtained through an iterative process using Eq. 1.2 until the desired value of the expansion ratio is reached:

$$\frac{1}{\varepsilon} = \left(\frac{k+1}{2}\right)^{\frac{1}{k-1}}\left(\frac{P_e}{P_c}\right)^{\frac{1}{k}}\sqrt{\frac{k+1}{k-1}\left[1-\left(\frac{P_e}{P_c}\right)^{\frac{k-1}{k}}\right]} \tag{1.2}$$

$$c^* = \frac{\sqrt{\frac{R}{M}T_c}}{\Gamma(k)} = 1560\,\frac{\mathrm{m}}{\mathrm{s}} \tag{1.3}$$

Some assumptions are here introduced:

- mono-phase mixture with frozen chemistry
- mono-dimensional expansion (quasi 1D gas dynamics)
- non-reactive flow
- isoentropic flow

Within the final assumption we also hypothesize that the fluid is non-viscous. The flow exit velocity is given by the following relation :

$$v_e = \sqrt{\frac{2k}{k-1}\frac{R}{M}T_c\left[1-\frac{p_e}{p_c}^{\left(\frac{k-1}{k}\right)}\right]} = 3022.0\,\frac{\mathrm{m}}{\mathrm{s}} \tag{1.4}$$

And it quickly follows that:

$$I_s = \frac{c^* c_T}{g_0} = 312.14\,\mathrm{s} \tag{1.5}$$

$$\dot{m}_p = \frac{T}{I_s g_0} = 0.0327\,\frac{\mathrm{kg}}{\mathrm{s}} \tag{1.6}$$

A bell-shaped nozzle was designed using the RAO approximation, in order to minimize the losses. Since there are no constraints on the weight of the nozzle a maximum length approach was used. Even though this choice makes the system heavier, we can expect an increase in the performance compared to a smaller, lighter one.
The geometrical properties of the RAO conical nozzle are shown below in Tab. 1.2.

Geometrical property	Value
Throat area [cm^2]	$A_t = \dfrac{T}{P_c C_F} = 0.2547$
Exit area [cm^2]	$A_e = \varepsilon\, A_t = 20.38$
Throat diameter [cm]	$d_t = 0.57$
Exit diameter [cm]	$d_e = 5.09$
Divergent angle [deg]	$\alpha = 15$
Convergent angle [deg]	$\beta = 45$
Characteristic length [m]	$L^* = 1.52$
Combustion chamber length [cm]	$L_{cc} = 25.33$

Table 1.2

The length of the divergent and convergent sections of the nozzle can be computed as:

$$L_{div} = \frac{1}{2}\frac{d_e - d_t}{\tan\alpha} = 8.43\,\mathrm{cm} \tag{1.7}$$

$$L_{conv} = \frac{1}{2}\frac{d_b - d_t}{\tan\beta} = 0.41\,\mathrm{cm} \tag{1.8}$$

Where d_b is the diameter of the combustion chamber determined considering a contraction ratio of $A_b/A_t = 6$ (see Appendix C.1). The length of the RAO nozzle is then equal to:

$$L_{\mathrm{nozzle}} = L_{conv} + L_{div} = 8.84\,\mathrm{cm} \tag{1.9}$$

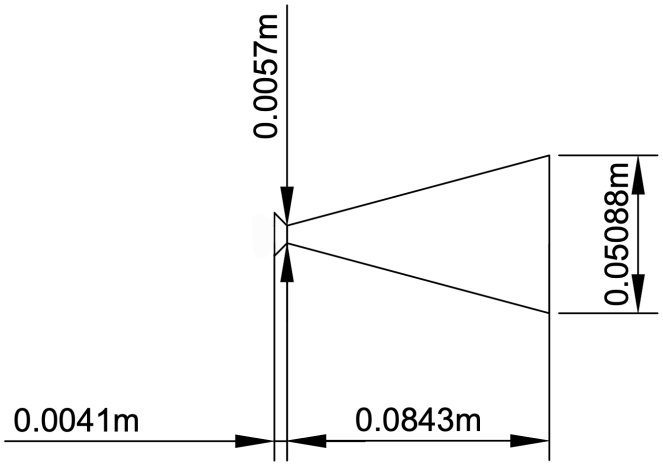

Figure 1.1: RAO Conical Nozzle (100 Newtons)

which, in return, in a maximum performance approach, is also equal to the length of the bell nozzle we are designing.
The initial and final angle of the parabolic approximation, θ_i and θ_e, are obtained graphically from the Rao curves and are equal to $\theta_i = 31.6°$, $\theta_e = 16.4°$, while the angle α of the divergent is the same as the conical reference nozzle. The losses in the nozzle are computed through Eq. 1.10.

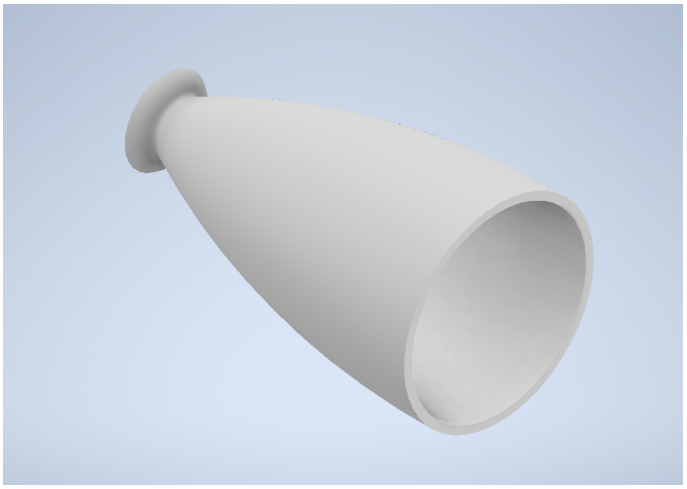

Figure 1.2: Qualitative sketch of the bell nozzle in scale (100 Newtons) - Autodesk Inventor

$$\lambda = \frac{1}{2}\left(1 + \frac{\alpha + \theta_e}{2}\right) \tag{1.10}$$

With this coefficient we can abandon the 1-D approximation and take into account the losses produced by the divergence of the flow, so that the real value of the thrust, of the specific impulse and of the thrust coefficient can be updated:

Parameter	Value
Thrust T_{real}	99.331 N
Specific Impulse $I_{s,real}$	313.65 s
Thrust coeff. $c_{T,real}$	1.9544

Table 1.3

1.2 Tank Sizing

Once the operating conditions of the engine are set, the sizing of the tanks becomes straightforward. First the propellant and oxidizer mass-flow rates are computed:

$$\dot{m}_{ox} = \frac{OF}{(1+OF)}\dot{m} = 0.0289\,\frac{\text{kg}}{\text{s}} \tag{1.11}$$

$$\dot{m}_{f} = \frac{1}{(1+OF)}\dot{m} = 0.0036\,\frac{\text{kg}}{\text{s}} \tag{1.12}$$

From these values and from the propellant densities the volumetric flows can also be calculated.
Taking into account a 5% margin for unused propellant and loading uncertainties, and a firing time of 100 s, the mass and volume of propellant needed can be determined as:

$$M_{ox} = \dot{m}_{ox}\, t_{burn}\, 1.05 = 3.030\,\text{kg} \tag{1.13}$$

$$M_{f} = \dot{m}_{f}\, t_{burn}\, 1.05 = 0.429\,\text{kg} \tag{1.14}$$

$$V_{ox} = \dot{V}_{ox}\, t_{burn}\, 1.05 = 2.2\,\text{L} \tag{1.15}$$

$$V_{f} = \dot{V}_{f} t_{burn} 1.05 = 0.53\,\text{L} \tag{1.16}$$

Similar margins will be considered when sizing the tanks, for instance to account for unusable volume.

Species	Density $\left[\frac{\text{kg}}{\text{m}^3}\right]$
H_2O_2 (OX)	1373
RP-1 (Fuel)	810

Table 1.4: Propellant compontents densities

To continue the design of the tanks, pressure losses need to be introduced:

- Feeding line losses (including the pressure drops across the valves) [0.3-0.5 atm].
- Injectors losses [$5 - 30\%$ of the combustion chamber pressure].
- Dynamic losses due to the flow velocity [v = 10 m/s].

The correct value of the overall pressure drop is identified and described in detail in the Off-design paragraph below, from it we can compute the initial pressure of each tank, assuming that it shall be equal to the nominal operating pressure of 20 bar of the combustion chamber, plus the amount of pressure lost along the feeding lines:

$$P_{tank,ox} = P_c + dP_{loss} = 35.82\text{ atm} \qquad P_{tank,f} = P_c + dP_{loss} = 25.67\text{ atm} \tag{1.17}$$

A blow-down system was developed during this work; to implement one, the pressurizing gas must share the same tank as the liquid, and it needs to be physically separated from the latter by a flexible bladder. For the pressurization of the engine it was selected Helium; assuming that its pressure is equal to the the pressure of the liquid phase inside each tank (see Appendix C.3). By looking for its thermo-chemical properties, and under the assumption of perfect gas, we can easily compute the volume that it will occupy and, subsequently, the overall volume of the two tanks. Furthermore, a safety margin of 10% on the whole volume shall be considered.

$$V_{tank,f} = 1.1\,(V_{fuel} + V_{in,He,f}) = 4.4\,\mathrm{L} \tag{1.18}$$

$$V_{tank,ox} = 1.1\,(V_{ox} + V_{in,He,ox}) = 7.9\,\mathrm{L} \tag{1.19}$$

Material density $\rho_{\text{tank}} = 8000\,\frac{\text{kg}}{\text{m}^3}$
Yield strength $\sigma = 500\,\text{MPa}$

By assuming two spherical tanks, it is possible to size their radii.
Furthermore, knowing the yield stress of the selected steel, and considering a safety margin on the rupture pressure of 2, such that $P_{blast} = 2P_{tank}$, the required thickness and, in the end, the mass of each tank is calculated.

	Radius [cm]	Thickness [mm]	Mass [kg]	$B = \frac{P_{in}}{P_{fin}}$
Oxidizer tank	12.36	0.9	1.385	2.73
Fuel tank	10.19	0.53	0.556	1.74

Table 1.5: Tanks data

1.3 Injection Plate Design

In order to model the injection plate we need to be able to evaluate the mass flow rate which has to pass though each injector.
For this purpose, consider these relations:

$$\dot{m} = C_d A \sqrt{2\Delta P_{inj}\rho} \tag{1.20}$$

$$v = C_d \sqrt{\frac{2\Delta P}{\rho}} \tag{1.21}$$

The parameters to be selected are:

- Pressure drop across the injector.
- Discharge coefficient.
- Diameter of the orifices.

The first unknown is related to the kind of injector while the second is connected to the shape of the orifices.

In this propulsion unit it is considered a configuration made of two injectors for oxidizer and one for the fuel, where each orifice is a short tube with conical entrance, from tables:

- $\Delta P_{inj} = 0.2 P_c = 4 \times 10^5$ Pa
- $C_d = 0.7 - 0.8$ (from the tables, iterated from the diameter of the orifice calculated)

The total injection mass flow rate is imposed and the required diameter of a single injector is then obtained. This procedure is possible thanks to the versatility of additive manufacturing and to impose the required initial conditions.

	Diameter [mm]	Number	$\dot{m}$ $\left[\frac{\text{kg}}{\text{s}}\right]$	v $\left[\frac{\text{m}}{\text{s}}\right]$	C_d
Oxidizer injector	0.824	2	0.0286	19.3	0.8
Fuel injector	0.537	1	0.0041	22	0.7

Table 1.6: Injector data

At this stage it is important to compute the discharge velocities of both the flows in order to confirm chocked conditions in the nozzle.

To simplify the design, a shower head configuration was chosen. This configuration is characterized by an axial flow velocity but a less efficient mixing of the oxidizer and fuel.

1.4 Manufacturing Process

The manufacturing process for this system will include extrusion, stamping and additive manufacturing (AM). Starting from the raw material, the design of the pipes and tanks will be made from AISI 316 stainless steel (SS) and externally purchased. The nozzle, combustion chamber and injection plate will all be made with Inconel alloy 718. Inconel 718 has been adopted in the space sector due to its strength, corrosion-resistance and production properties in normal manufacturing methods. For the case analysed, the production will be done through AM techniques that, in addition to Inconel's proven success, show promise in terms of production time, material usage and potential added benefits to metallurgic properties. (Jia and Gu, 2014)

1.4.1 Additive Manufacturing

The additive manufacturing method chosen for the design of the components is the Selective Laser Melting (SLM) process, which allows the production of highly complex internal and external features. SLM is suitable for the construction of parts in the micro meter size and it is ideal for a a unit like the one designed. (Gradl et al., 2018)
The 20-100 μm laser resolution translates to a surface roughness and uncertainty in the linear measurements. (Oztan and Coverstone, 2021)
The uncertainty is around 0.1 mm and is one of the main issues together with the residual powder deposition. Although there are other relevant AM processes, SLM has post process solutions that give an overall advantage. SLM can be paired with other post process methods such the pickling process, or the more traditional ones such as turning, milling and boring processes to solve such problems. (Metal supermarkets, 2022) To avoid powder deposition, one solution is to make the grains average diameter smaller, in order to decrease the amount of residual powder stuck to the piece during the process. Pair this with a higher heat input of a higher laser power, and a lower scanning rate will more efficiently melt the powder particles. However it is necessary to find a good compromise since a high heat input generally decreases the surface roughness but it could also result in

an increase of the latter due to high thermal stresses and non-uniform solidification rate. From the nozzle point of view, it is necessary to point out that, since it has a bell shape, it is subjected to the "stair step effect", due to the stepped approximation by layers of curved and inclined surfaces. The effect is shown graphically in Figure 1.3.

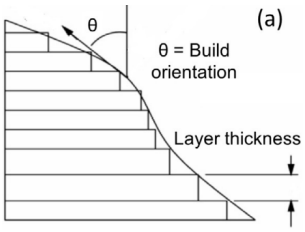

Figure 1.3: Stair step effect

$$R_a = 1000\, t_l \sin\frac{90-\theta}{4} \tan(90-\theta) \tag{1.22}$$

As the formula shows, to improve this issue, the step size of the thickness layer, t_l, can be reduced, at the cost of incrementing the time of the process, so a good compromise is needed to be found. (DebRoy et al., 2018)

10 N and 1000 N thrust engines: uncertainties effects and main design aspects

By following the same principles showed in the nominal configuration with RAO approximation we can size the nozzles in the 10 and 1000 N cases (see Appendix C.3 on page 17). Scaling up the engine in order to deliver a 1000 N thrust does not represent a problem from a manufacturing point of view; it is safe to assume that the order of magnitude of the uncertainties does not change by enlarging the system and, therefore, does not affect the overall performance in any particular way. On the other hand, the realization of a 10 N thruster must face the problem of manufacturing even smaller parts than the one already implemented for the nominal engine. Additive manufacturing cannot be considered for these applications, since the size of the injectors can become comparable to its uncertainties. Moreover, from a heat-transfer point of view, by miniaturizing the system we are effectively reducing the flow-rate which implies less cooling in the cooling system. The small amount of material involved in miniaturized thrusters presents lower capabilities of heat transfer. Another key aspect is represented by pressure: smaller diameters reflect into high operating pressures, raising the difficulties in cooling due to higher heat transfer coefficient.

Monte Carlo Simulation 2

The Monte Carlo simulation [include appendix section for Monte Carlo explanation] is a common process used for statistical analysis of different possibilities in the results of the system being analyzed. In this case, the simulation result range in thrust and mass flow rate will be affected by the geometry uncertainty.

2.1 Uncertainties

A list of uncertainties were compiled accounting for the uncertainties mentioned in the manufacturing process. Recall that the resolution of the selected AM processes range between 20-100 microns, as decribed in Appendix B on page 15. Choosing 100 microns as the maximum deviation ($4\sigma_U$) from nominal gives the range of the geometric uncertainty. Accounting for the sizing values of the system, the most effected dimensions shall be the throat area of the nozzle and the area of the injector plate holes. The nominal nozzle throat radius and injector plate oxidizer and fuel hole radii are presented in Table 1.2 on page 2 and Table 1.6 on page 6, respectively. The nozzle throat and injector plate holes, in proportion to the propulsion unit geometry, are much smaller, so the rest of the propulsion unit geometry is considered static at nominal values, such as the nozzle diameter, length, combustion chamber area, pressure, ext. The assumption to make the throat radius and injector hole radius variable is because they are at the order of magnitudes closest to the manufacturing uncertainties and therefore have the greatest impact on the propulsion system results. The decision to leave the other variables static is made because the effects are assumed negligible as well as it reduces the complexity of calculations.

2.2 Results

The Monte Carlo simulation was run for 500 iterations in order to reach a reasonable convergence on the thrust, combustion chamber pressure, and propellant mass flow rate. The results from the Monte Carlo simulation are shown in Figure 2.1 to 2.3 on the following page. Viewing the Monte-Carlo simulation, it is evident that the results converge to reasonable values, although not nominal values. The thrust cumulative mean in Figure 2.1a converges to a value of roughly 99 N which is within one percent of the nominal value. One reason a convergence for this deviation is due to a tabulated value for the discharge coefficients for both the oxidizer and the fuel. This reasoning applies across all the values calculated I.e. pressure and mass flow rate. The standard deviation is roughly 7-8% for each variable compared to the nominal values. The standard deviation value indicates that the variables, nozzle throat radius and injector plate hole radii, affect the system performance parameters to a significant degree.

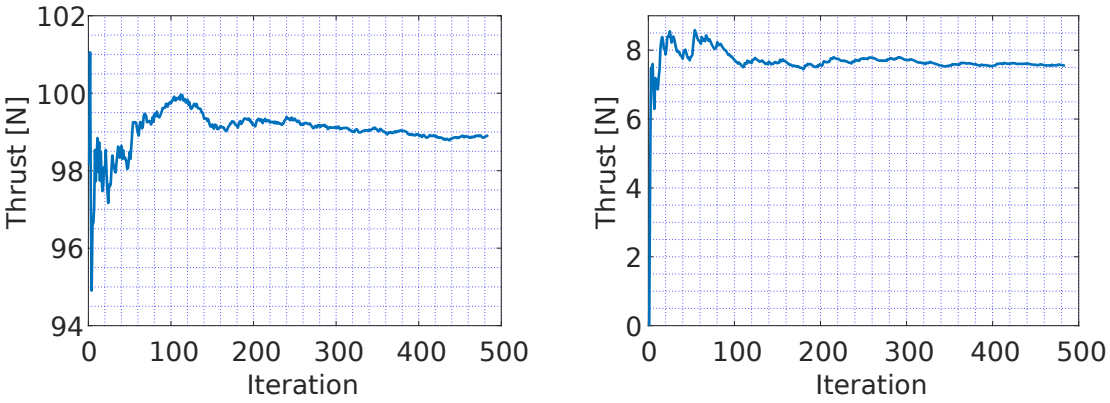

(a) Thrust cumulative mean **(b)** Thrust standard deviation

Figure 2.1: Thrust results

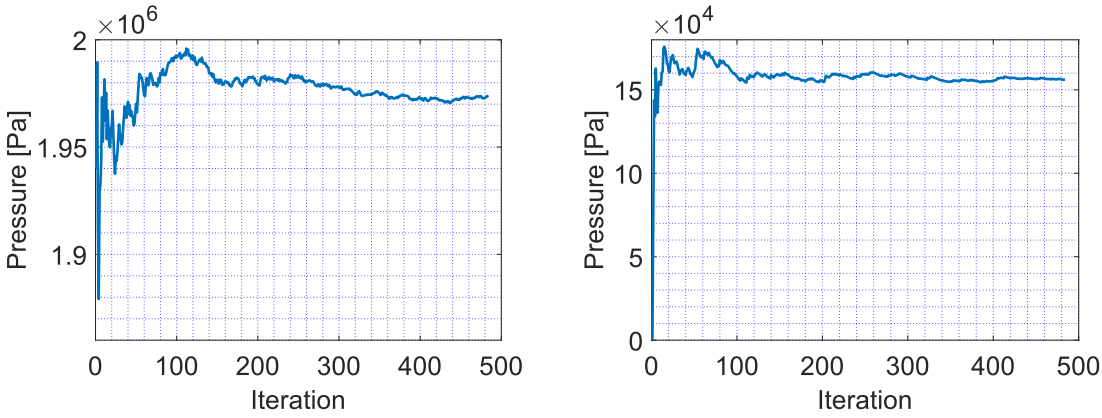

(a) Combustion chamber pressure cumulative mean **(b)** Combustion chamber pressure standard deviation

Figure 2.2: Combustion chamber pressure results

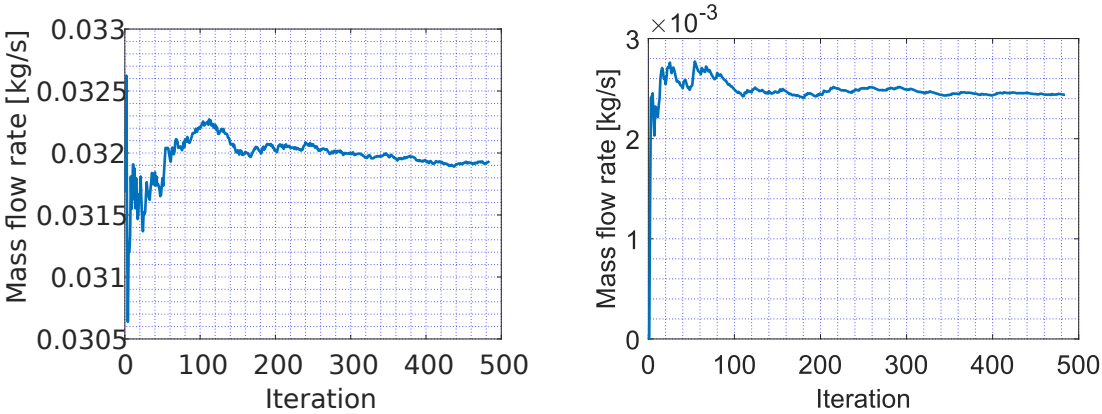

(a) Mass flow rate cumulative mean **(b)** Mass flow rate standard deviation

Figure 2.3: Mass flow rate results

Off-design performances 3

As the system does not use flow regulating valves, the blow-down configuration causes a drop of the pressure in the combustion chamber during the firing, due to the progressively lower tank pressure. This creates a decrease in thrust and specific impulse. To respect the requirements on the minimum thrust level, a simulation of the behaviour and an accurate design of the pressurizer volume must be made.

3.1 Feeding line model

In order to simulate the behaviour of the system is necessary to consider all pressure losses in the line from the tanks up to the combustion chamber. These losses are related to the mass flow rate, that is imposed from the difference in pressure across the line. The pressure losses in the line are divided in distributed and concentrated. The distributed losses were modeled assuming a constant friction factor $f = 0.015$, using the formula:

$$\Delta p = \frac{\rho f L v^2}{D_{line}} \tag{3.1}$$

where ρ and and v are the density and velocity of the fuel, L is the length of the line, and D is the diameter of the pipes.(Sellens, 2022) The concentrated pressure losses, two different models were used for the valves and the injectors, for the valves the difference of pressure was calculated as:

$$\Delta p = \frac{1}{2}\rho K v^2 \tag{3.2}$$

Where K is function of K_v, obtained from the formula:

$$K_v = q_v \sqrt{\frac{10^2 \rho}{\Delta p}} \tag{3.3}$$

substituting the volumetric flow rate $q_v = \frac{\pi D^2 v}{4}$. And converting between m^3/h and kg/s. (KOSO PARCOL S.r.l., 2022)
In our case we used $K_v = 4$ for our valves.

For the injection plate, the valve loss formula was used, calculating K from the discharge coefficient as:

$$K = \left(\frac{D_{line}^2}{n_{inj} d_{inj}^2 C_d} \right)^2 \tag{3.4}$$

Derived from the formula of the pressure losses across an orifice.

3.2 Iterative process flow

Performing an iterative process it is possible to compute the evolution of the system during time. During each time step it is necessary to take some parameters from the previous step in order to compute the new value. In this case the characteristic velocity and mass flow rate from the previous iteration were chosen to calculate the pressure in the combustion chamber. From this value, knowing the pressure in the tanks, calculated using a isothermal expansion, the pressure drop across the line was calculated and thus the mass flow rate required to have that drop. The characteristic velocity was calculated from the thermodynamic data from NASA CEA code, interpolated over a range of O/F and P_c values.

Knowing the characteristic velocity, thrust coefficient and mass flow rate, the thrust profile, specific impulse and other performance parameters were recovered. From these data, the necessary initial volume of pressurizer needed inside the tanks to maintain a level of thrust higher than 50% of the initial value was chosen. This is because, during the burn, the smaller the volume of the pressurizer, the higher the pressure change in the tanks, and thus in the combustion chamber, would be.

The values chosen are: $V_{press,ox} = 0.005\,\mathrm{m}^3$, $V_{press,fu} = 0.0035\,\mathrm{m}^3$ These values are reasonable but actually bigger than necessary, this choice was made to minimize the performance drop during the burn.

3.3 Results

As expected the configuration of the system leads to a reduction in performance during the firing time. In particular, with the values chosen for the pressurizing gas we can observe a reduction of the pressure in the combustion chamber from 20 bar (nominal condition) to about 16 bar. This is linked to a reduction of the propellant mass flow rate, but, as we can see from Figure 3.1 (e), as the oxidizer mass flow rate decreases, the fuel mass flow rate increase slightly. As a result the OF ratio decreases progressively. All these aspects contribute to the overall performance of the motor, so both specific impulse and thrust are reduced. In particular the thrust at the end of the burning time is equal to 79,95 N: the requirement about the thrust is satisfied. All the results are summarized in the figures below.

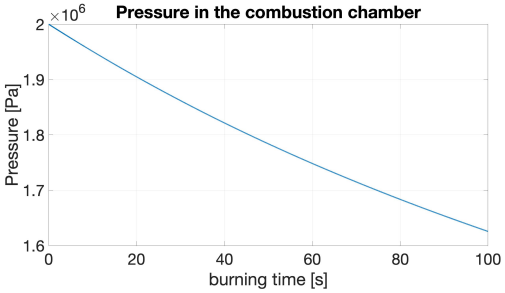

(a) Pressure in combustion chamber

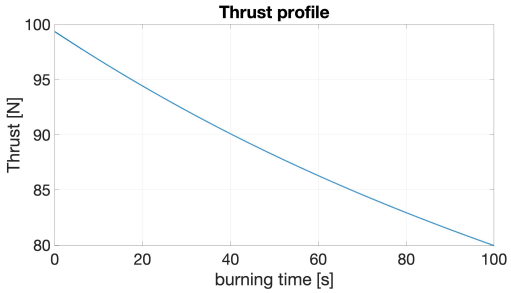

(b) Thrust profile during the burn

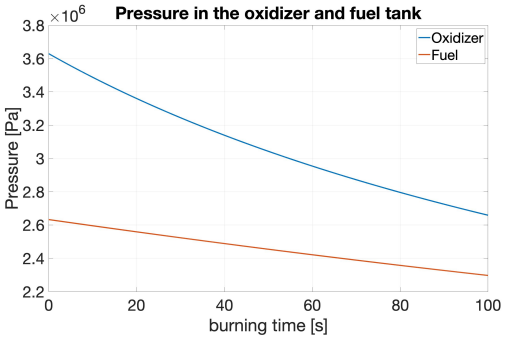

(c) Pressure in oxidizer and fuel tanks

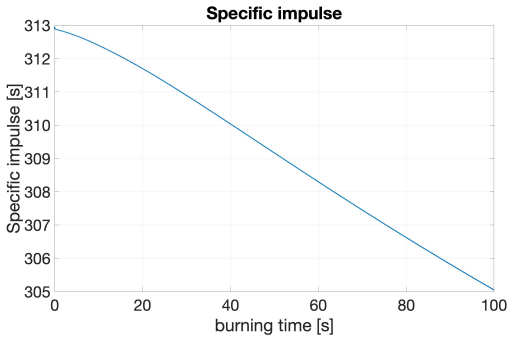

(d) Specific impulse progression

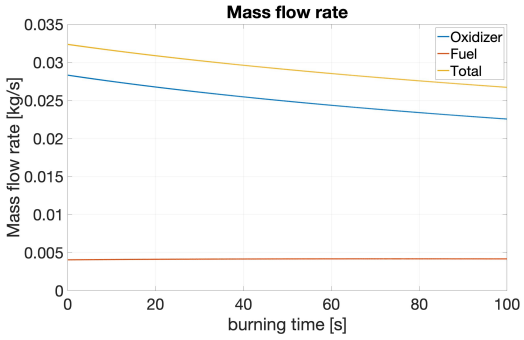

(e) Mass flow rate progression

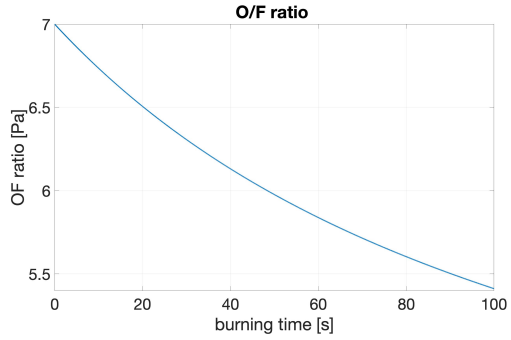

(f) OF ratio progression

Figure 3.1: Performance parameter progression

Bibliography

Literature

DebRoy, T. et al. (2018). "Additive manufacturing of metallic components – Process, structure and properties". In: *Progress in Materials Science* 92, pp. 112–224. ISSN: 0079-6425. DOI: https://doi.org/10.1016/j.pmatsci.2017.10.001. URL: https://www.sciencedirect.com/science/article/pii/S0079642517301172.

Gradl, Paul et al. (July 2018). "Additive Manufacturing of Liquid Rocket Engine Combustion Devices: A Summary of Process Developments and Hot-Fire Testing Results". In: DOI: 10.2514/6.2018-4625.

Jia, Qingbo and Dongdong Gu (2014). "Selective laser melting additive manufacturing of Inconel 718 superalloy parts: Densification, microstructure and properties". In: *Journal of Alloys and Compounds* 585, pp. 713–721. ISSN: 0925-8388. DOI: https://doi.org/10.1016/j.jallcom.2013.09.171. URL: https://www.sciencedirect.com/science/article/pii/S0925838813023451.

Oztan, Cagri and Victoria Coverstone (2021). "Utilization of additive manufacturing in hybrid rocket technology: A review". In: *Acta Astronautica* 180, pp. 130–140. ISSN: 0094-5765. DOI: https://doi.org/10.1016/j.actaastro.2020.11.024. URL: https://www.sciencedirect.com/science/article/pii/S0094576520307001.

Websites

KOSO PARCOL S.r.l. (2022). *HANDBOOK FOR CONTROL VALVE SIZING*. URL: https://www.parcol.com/docs/ACA0101_gb.pdf (visited on 05/21/2022).

Metal supermarkets (2022). *What is Steel Pickling?* URL: https://www.metalsupermarkets.com/what-is-steel-pickling/ (visited on 05/21/2022).

Sellens, Rick (2022). *Losses in Pipes*. URL: https://me.queensu.ca/People/Sellens/LossesinPipes.html (visited on 05/21/2022).

Assignment details A

The purpose of this document is to discuss the development of a new storable liquid propulsion system.

The work will be mainly focused on the design of a 100 N thrust engine characterized by the following:

Property	Description
Propulsion unit kind	Bi-Propellant
Oxidizer	Hydrogen peroxide $H_2 = O_2$ (87.5%)
Propellant	RP-1
Architecture	Blow-Down
Combustion chamber material	Inconel 718
Tanks and pipes material	Stainless steel AISI 316
Expansion ratio ϵ	80
Hydraulic system	Open-close valve and check valve for each feeding line

The project is divided into four phases:

- design of the overall system in the nominal configuration;
- characterization of the propulsion parameters during the firing, as function of the time;
- critically revision of the design from the realization viewpoint;
- discussion on the most critical sources of uncertainties for the nominal thrust level and, only qualitatively, for a down-scaling of the technology to smaller thrust.

Additive manufacturing B

Additive Manufacturing (AM) is a process that has significantly matured in last years. In particular for Liquid rocket engine, this process is widely used because of it reduces noticeably hardware costs, increases reliability by reducing the number of joints and improves hardware performance by allowing fabrication of designs not feasible by conventional process. The most common additive manufacturing process for aerospace application is the Selective Laser Melting method (SLM). It uses a layer-by-layer powder-bed approach in which the desired component features are sintered and subsequently solidified using a laser and it allows to fabricate complex internal and external features. Using AS for the chamber injection plate reduces production costs because it does not need to deal with the traditional reductive manufacturing of parts and their assembly processing. With these benefits come some disadvantages, particularly regarding the roughness of the manufactured piece caused by improper melting of the power. To mitigate this problem, higher heat input and low scanning speed can be selected to improve the sintering of the powder. Average powder diameter itself is an important parameter because it is proportional to roughness. Smaller diameters reduce surface roughness and facilitate melting. Despite that, SLM isn't a net shape process (tolerance in the range of 20 µm to 100 µm) and usually requires other processes to reach higher quality surface finish (chemical process, material removal processes etc. etc.). (Gradl et al., 2018; DebRoy et al., 2018)

Relevant design data C

C.1 Specific impulse vs Oxidizer to fuel ratio

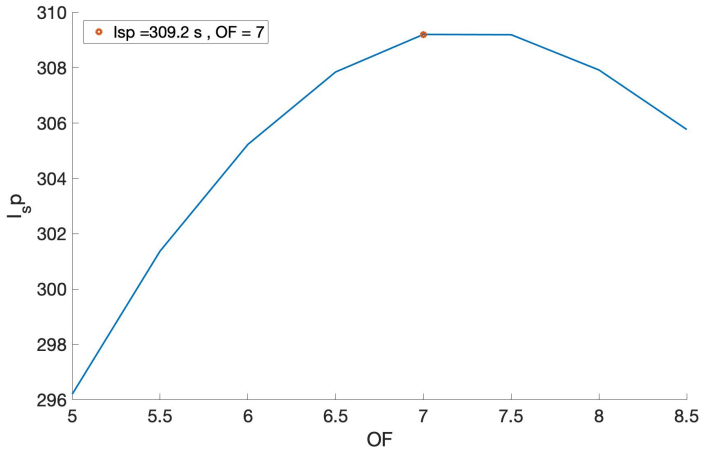

Figure C.1: I_s vs OF

C.2 Combustion Chamber

Note that, by assuming a Mach number in the combustion chamber between 0.2 – 0.4, the area of such subsystem can be computed as

$$A_{cc} = \frac{A_t}{M_c}((\frac{2}{k+1})(1+\frac{k-1}{2}M_c^2))^(\frac{k+1}{2(k-1)}) = 0.77\,\mathrm{cm}^2; \tag{C.1}$$

With the data in our possession this correspond to a contraction ratio of 3. From Sutton book we can assume a characteristic length of the combustion chamber,$L^* = 1.52$, from which the volume and the length of the chamber itself can be computed:

$$V_{cc} = L^* A_t = 0.039\,\mathrm{L} \tag{C.2}$$

$$L_c = \frac{V_{cc}}{A_{cc}} = 50.1\,\mathrm{cm} \tag{C.3}$$

As one can notice, in this configuration the combustion chamber appears very thin and long, which is why we decided to impose the contraction ratio instead. Ac = 6*At = 1.53 cm2 This will result in a penalty from the mass point of view, penalty that falls beyond the scope of this assignment and will not be further discussed.

C.3 10 N and 1000 N thruster data

Following the same workflow adopted for the nominal design, the geometry of the thrust chamber of the 10 and 1000 N scaled thrusters is here reported: **Bell-nozzles shape** is considered and again designed through RAO approximation with the parameters showed below:

10 N thruster

Geometrical property	Value
Nozzle length[m]	$L_{nozzle,10N} = 0.028$
Throat area [m^2]	$A_t = \frac{T}{P_c C_F} = 2.5412e-06$
Exit area[m^2]	$A_e = \varepsilon\, A_t = 2.0330e-04$
Throat diameter[m]	$d_t = 0.0018$
Exit diameter[m]	$d_e = 0.0161$
Divergent part angle [deg]	$\alpha = 15$
Convergent part angle [deg]	$\beta = 45$

1000 N thruster

Geometrical property	Value
Nozzle length[m]	$L_{nozzle,1000N} = 0.28$
Throat area [m^2]	$A_t = \frac{T}{P_c C_F} = 2.5412e-04$
Exit area[m^2]	$A_e = \varepsilon\, A_t = 0.0203$
Throat diameter[m]	$d_t = 0.0180$
Exit diameter[m]	$d_e = 0.1609$
Divergent part angle [deg]	$\alpha = 15$
Convergent part angle [deg]	$\beta = 45$

C.4 Pressurizing gas

R [$\frac{\text{J}}{\text{kg K}}$]	K	ρ [$\frac{\text{kg}}{\text{m}^3}$]	T [K]
2076.9	1.667	0.178	298.15

Table C.1: Helium properties